Acute regulation of aquaporin-2 phosphorylation at Ser-264 by vasopressin

Robert A. Fenton*†, Hanne B. Moeller*, Jason D. Hoffert‡, Ming-Jiun Yu‡, Søren Nielsen*, and Mark A. Knepper‡

*The Water and Salt Research Center, Institute of Anatomy, University of Aarhus, DK-8000 Aarhus C, Denmark; and ‡Laboratory of Kidney and Electrolyte Metabolism, National Heart, Lung, and Blood Institute, National Institutes of Health, Bethesda, MD 20892

Communicated by Peter C. Agre, Duke University, Durham, NC, December 29, 2007 (received for review November 22, 2007)

By phosphoproteome analysis, we identified a phosphorylation site, serine 264 (pS264), in the COOH terminus of the vasopressin-regulated water channel, aquaporin-2 (AQP2). In this study, we examined the regulation of AQP2 phosphorylated at serine 264 (pS264–AQP2) by vasopressin, using a phospho-specific antibody (anti-pS264). Immunohistochemical analysis showed pS264–AQP2 labeling of inner medullary collecting duct (IMCD) from control mice, whereas AQP2 knockout mice showed a complete absence of labeling. In rat and mouse, pS264–AQP2 was present throughout the collecting duct system, from the connecting tubule to the terminal IMCD. Immunogold electron microscopy, combined with double-labeling confocal immunofluorescence microscopy with organelle-specific markers, determined that the majority of pS264 resides in compartments associated with the plasma membrane and early endocytic pathways. In Brattleboro rats treated with [deamino-Cys-1, D-Arg-8]vasopressin (dDAVP), the abundance of pS264–AQP2 increased 4-fold over controls. Additionally, dDAVP treatment resulted in a time-dependent change in the distribution of pS264 from predominantly intracellular vesicles, to both the basolateral and apical plasma membranes. Sixty minutes after dDAVP exposure, a proportion of pS264–AQP2 was observed in clathrin-coated vesicles, early endosomal compartments, and recycling compartments, but not lysosomes. Overall, our results are consistent with a dynamic effect of AVP on the phosphorylation and subcellular distribution of AQP2.

concentrating mechanism | immunohistochemistry | kidney | trafficking

The maintenance of body water homeostasis depends on the fine control of renal water excretion, a process that is regulated by the antidiuretic hormone arginine vasopressin (AVP). An essential step in the action of AVP is the trafficking of intracellular vesicles containing the AVP-sensitive water channel aquaporin-2 (AQP2) to the plasma membrane of kidney collecting duct (CD) principal cells, a process that ultimately increases osmotically driven water reabsorption from the CD lumen and the production of concentrated urine (1). After small increases in plasma osmolality, AVP is released by the posterior pituitary gland and binds to the type II AVP receptor (V2R) in the CD, leading to activation of adenylyl cyclase, increased intracellular cAMP levels, increased intracellular calcium, and activation of PKA. Numerous studies, in both cell culture and animal models, suggest that PKA phosphorylation of serine 256 (S256) in the COOH tail of AQP2 plays a critical role in its apical trafficking (2–5). In addition to S256, we have discovered recently that AQP2 is further phosphorylated on residues S261, S264, and S269 in the COOH tail in response to AVP stimulation (6, 7).

In this study, we examined the regulation of AQP2 phosphorylated at serine 264 (pS264–AQP2) by AVP in a number of *in vivo* models by using a phospho-specific antibody. Our findings demonstrated that pS264–AQP2 abundance is regulated acutely by AVP and that pS264–AQP2 appears in both the basolateral and apical membrane of the CD in a time-dependent manner. Additionally, AVP stimulation, followed by agonist removal, resulted in the appearance of pS264–AQP2 in early endosomes, but not in lysosomes, suggesting that phosphorylation at this residue may influence intracellular compartmentalization of AQP2 after endocytosis or that the enzymes that phosphorylate or dephosphorylate AQP2 at S264 are compartment-specific.

Results

Cellular and Subcellular Distribution of pS264–AQP2. Immunolabeling of normal rat kidney sections determined that pS264–AQP2 was weakly expressed in all regions of the CD [Fig. 1 and supporting information (SI) Fig. 10], with approximately equal labeling intensities between the kidney regions. A similar pattern was observed in normal mouse kidney, but labeling intensity was greater. In both species, labeling was predominantly localized in the apical or subapical domain (Fig. 1, insets), with very little labeling of the basolateral membrane domain. A complete absence of CD labeling in AQP2 knockout mice showed that the anti-pS264 antibody was specific for AQP2 (Fig. 1 *E* and *F* and SI Fig. 11). Furthermore, pS264 labeling was ablated when the antibody was preadsorbed with a synthetic COOH-terminal pS264–AQP2 phosphopeptide but not with a similar unphosphorylated AQP2 peptide (Fig. 1 *G* and *H*), indicating that the labeling is specific for AQP2 phosphorylated at residue S264. Double immunofluorescence labeling with the connecting tubule (CNT) cell marker calbindin (Fig. 2*A*) or the intercalated cell marker H^+-ATPase (Fig. 2*B*) showed that pS264 is weakly expressed in CNT and within the CD is restricted to principal cells (SI Fig. 12). Immunolabeling in mice showed a similar distribution (data not shown). Double immunofluorescence labeling with an NH_2-terminal total AQP2 antibody showed a high degree of colocalization ($R_{coloc} = 0.78 \pm 0.10$) between pS264 and total AQP2 in all CDs (Fig. 2*C*), with colabeling mainly observed at the apical plasma membrane and subapical domains. Higher magnification (Fig. 2*D*) demonstrated that total AQP2 (shown in red) was more broadly distributed than pS264, especially in the basolateral membrane domains.

A qualitative analysis of normal rat kidneys by immunogold electron microscopy revealed that in CD principal cells, pS264 is observed in subapical vesicles and the apical plasma membrane domain (Fig. 3*A*). Additionally, pS264 is detected in numerous other intracellular "vesicles". After short-term [deamino-Cys-1, D-Arg-8]vasopressin (dDAVP) treatment (30 min), the abundance of pS264 clearly increased in the apical plasma membrane (Fig. 3*B*), but numerous gold particles were still observed intracellularly. Additionally, after AVP treatment for this time period, a few gold particles were also observed in the basolateral membrane domains (data not shown). Although our current observations are qualita-

Author contributions: R.A.F., H.B.M., and M.A.K. designed research; R.A.F., H.B.M., J.D.H., and M.-J.Y. performed research; J.D.H. and M.A.K. contributed new reagents/analytic tools; R.A.F., H.B.M., J.D.H., S.N., and M.A.K. analyzed data; and R.A.F., H.B.M., S.N., and M.A.K. wrote the paper.

The authors declare no conflict of interest.

†To whom correspondence should be addressed at: The Water and Salt Research Center, Institute of Anatomy (Building 233), University of Aarhus, DK-8000 Aarhus, Denmark. E-mail: rofe@ana.au.dk.

This article contains supporting information online at www.pnas.org/cgi/content/full/0712338105/DC1.

www.pnas.org/cgi/doi/10.1073/pnas.0712338105

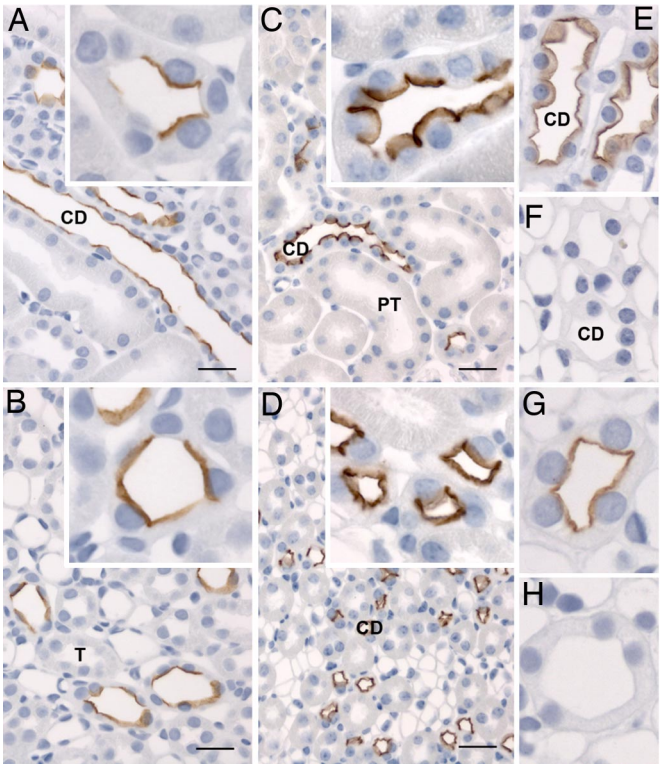

Fig. 1. Immunoperoxidase labeling of pS264–AQP2 in normal kidney. (*A* and *B*) Weak labeling of pS264 is evident in all regions of the CD in normal rat kidney [cortex (*A*) and inner stripe of outer medulla (*B*)]. (*A* and *B Insets*) At high magnification, labeling is predominantly apical membrane-associated, with some intracellular staining. (*C* and *D*) A similar pattern of labeling is observed in normal mouse kidney [cortex (*C*) and inner stripe of outer medulla (*D*)], with labeling restricted to the apical membrane domains (*Insets*). (*E* and *F*) AQP2 knockout mouse (*F*) shows a complete absence of p264 labeling compared with control mouse (*E*). (*G* and *H*) Preabsorption of anti-pS264 with nonphosphorylated peptide (*G*) or pS264 peptide (*H*) indicates that labeling is specific for the pS264–AQP2. T, thick ascending limb; PT, proximal tubule. (Scale bars, 20 μm.)

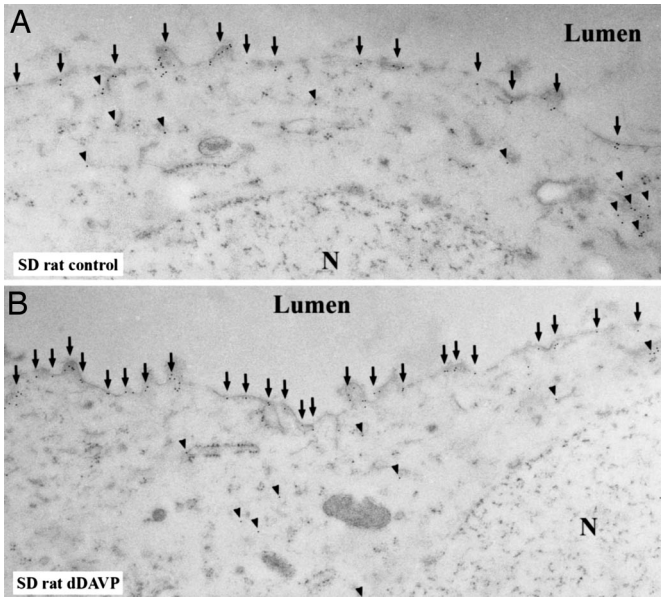

Fig. 3. Immunoelectron microscopy of pS264–AQP2 in normal rat kidney. (*A*) In rat kidney collecting duct principal cells, immunogold labeling of pS264 is observed intracellularly (arrowheads) and in the apical plasma membrane domains (arrows). (*B*) After dDAVP treatment (30 min), the number of gold particles increases in the apical plasma membrane (arrows), but intracellular gold can still be observed (arrowheads). N, nucleus.

tive, they do suggest that there is a large increase in pS264 abundance in the apical plasma membrane after dDAVP exposure.

To define the subcellular distribution of pS264–AQP2, double immunofluorescence labeling was performed with subcellular markers. Little colocalization was observed with pS264 and the endoplasmic reticulum (ER) marker protein disulphide isomerase (PDI), the medial Golgi marker *GS28*, the *cis*-Golgi marker p115, and the *trans*-Golgi network (TGN) marker *Vti1a* (Fig. 4 and SI Table 1). Some colocalization was observed in some tubules with the early endosome marker EEA1, the clathrin-coated vesicle marker adaptin-G, and the recycling endosome marker Rab11 (Fig. 4), suggesting that, under normal conditions, the majority of pS264 resides in compartments associated with the plasma membrane and early endocytic pathways (SI Fig. 13). No colocalization was observed with the lysosomal marker cathepsin D (Fig. 4) or the late endosome marker mannose-6-phosphate (data not shown).

Effect of Short-Term Vasopressin Treatment on pS264 Abundance. To determine the effects of short-term AVP treatment on pS264 abundance *in vivo*, semiquantitative immunoblotting was performed on inner medulla protein homogenates isolated from either AVP-deficient Brattleboro rats or normal Sprague–Dawley rats treated with the V2R-selective vasopressin analog dDAVP (Fig. 5). In both models, the total abundance of AQP2 was not changed in

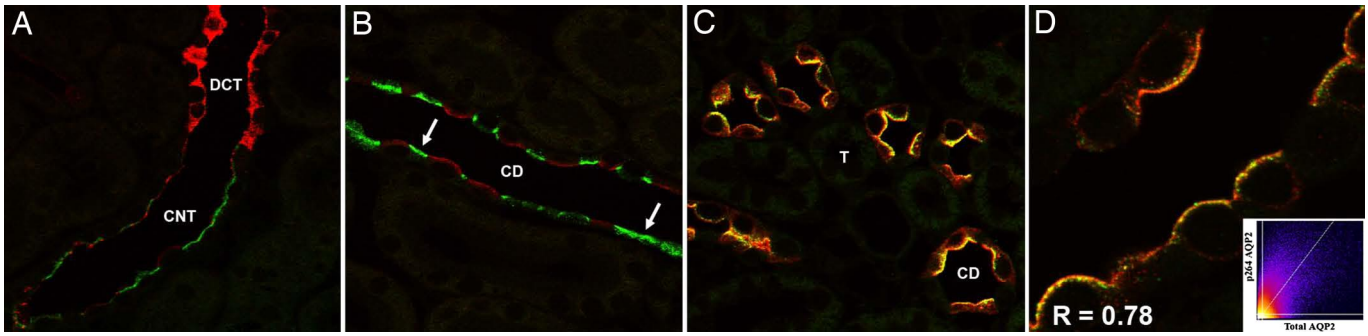

Fig. 2. Confocal laser-scanning microscopy of pS264–AQP2 in normal rat kidney. (*A*) Double immunofluorescence labeling of pS264 (green) and calbindin (red) identified pS264 in connecting tubules. (*B*) Double immunofluorescence labeling of p264 (green, arrows) and [H^+]ATPase (red) determined that pS264 is expressed in collecting duct principal cells. (*C*) Total AQP2 (red) and pS264 (green) colocalize (yellow) in collecting duct. (*D*) Higher magnification shows a high degree of correlation (depicted in histogram, inset) between total AQP2 and pS264 [Pearson correlation coefficient (*R*) in the colocalized volume, 0.78]. DCT, distal convoluted tubule.

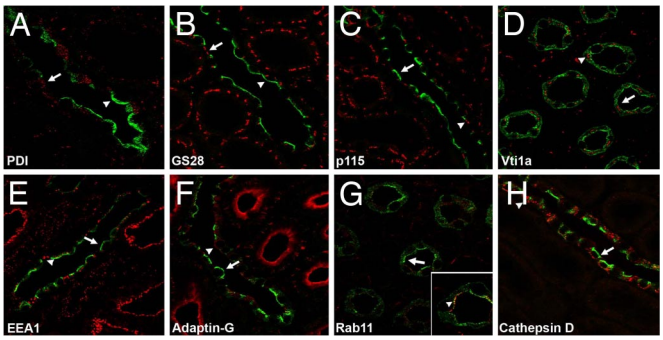

Fig. 4. Subcellular distribution of pS264–AQP2 in normal rat kidney collecting duct. For all images, pS264 is depicted in green, the specific intracellular marker is depicted in red, and the overlaid images show colocalized pixels in yellow, with arrows indicating pS264 and arrowheads indicating the intracellular compartment. Little colocalization is observed with the ER marker PDI (*A*), the medial Golgi marker GS28 (*B*), the *cis* Golgi marker p115 (*C*), and the TGN marker Vti1a (*D*). Some colocalization is observed in some tubules with the early endosome marker EEA1 (*E*), the clathrin-coated vesicle marker adaptin-G (*F*), and the recycling endosome marker Rab11 (*G*). No colocalization is observed with the lysosomal marker cathepsin D (*H*). See SI Table 1 for statistical comparison.

response to 30 min of dDAVP treatment. In contrast, the levels of AQP2 phosphorylated at S256 and S264 increased significantly, indicating that phosphorylation of AQP2 at both these sites can be regulated acutely by AVP. Additionally, a time course study of dDAVP effects in Brattleboro rats (20, 40, 80 min) determined that pS264 abundance reached a maximum at 20 min and remained elevated thereafter (data not shown).

Short-Term Vasopressin Treatment Results in Increased pS264–AQP2 in the Basolateral and Apical Membrane Domains. To investigate whether the increased pS264 abundance after short-term dDAVP treatment was associated with an altered distribution within the CD, we initially analyzed pS264 localization in kidney sections isolated from Brattleboro rats 30 min after a single dose of dDAVP. In untreated controls, weak intracellular labeling of pS264 was evident in all kidney zones (Fig. 6 *A–C* and SI Fig. 14). Thirty minutes after dDAVP exposure, pS264 labeling increased in intensity predominantly at the apical plasma membrane (Fig. 6 *D–F*). In some outer medullary CDs, and throughout the inner medullary CD (IMCD), increased basolateral plasma membrane labeling was observed. Additionally, in the majority of IMCD cells small vesicle structures were labeled in the subapical membrane domain (data not shown). In comparison, total AQP2 has highly abundant intracellular labeling throughout the kidney CD before dDAVP exposure (Fig. 6 *G–I*). Upon stimulation, the abundance of AQP2 labeling was not increased, but clear translocation of AQP2 to the apical membrane, and to the basolateral plasma membrane domains in the IMCD, could be observed (Fig. 6 *J–L*).

To further explore the acute effect of AVP on pS264–AQP2 distribution, confocal laser scanning microscopy was performed on kidney sections isolated from Brattleboro rats administered either saline (control) or dDAVP for 15 or 60 min (Fig. 7). Urine osmolalities under these conditions were 164 ± 18, 224 ± 4, and 800 ± 86 mosmol/kg H_2O for control and 15- and 60-min dDAVP, respectively. By using this technique, distinct dispersed pS264-labeled intracellular vesicles could be identified (Fig. 7*A*). Fifteen minutes after a single injection of dDAVP, this dispersed pS264 labeling completely disappeared and was replaced by strong labeling throughout the CD on both the apical plasma membranes and the basolateral membrane domains (Fig. 7*B*). The increase in basolaterally associated pS264 labeling was much more apparent in the inner medulla but could also be observed in other kidney zones (data not shown). Sixty minutes after dDAVP injection, pS264 was predominantly associated with the apical plasma membrane, although some basolateral labeling was still observed. Additionally, punctate staining of intracellular structures could be observed throughout CD principal cells (Fig. 7*C*, inset).

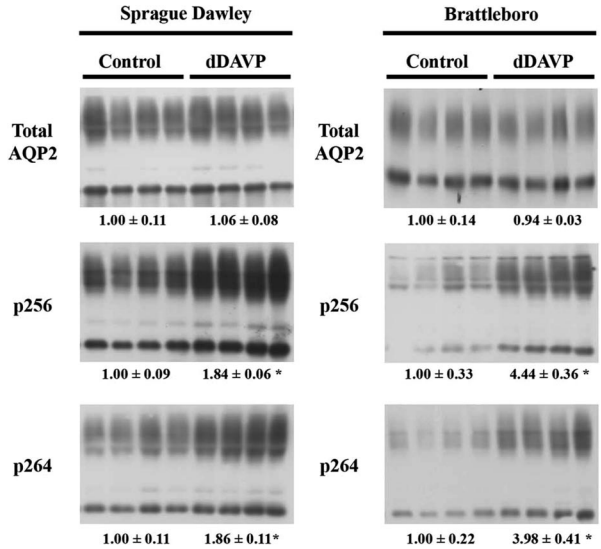

Fig. 5. The abundance of pS264–AQP2 is increased with short-term vasopressin exposure. Immunoblots assessing relative total AQP2, pS256, and pS264 abundance in inner medulla homogenates from Sprague–Dawley rats or Brattleboro rats after dDAVP treatment (30 min). Each lane was loaded with a sample from a different rat. The values are mean band densities normalized such that the mean for the control rats is defined as 1. *, Significant change in mean band densities among groups.

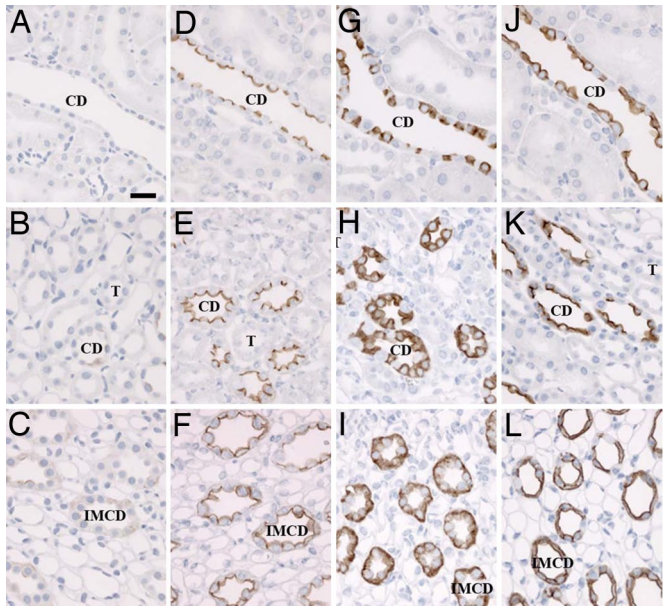

Fig. 6. Short-term vasopressin exposure increases pS264–AQP2 abundance at the plasma membrane. (*A–C*) Weak intracellular labeling of pS264 is evident in Brattleboro rat kidney cortex (*A*), inner stripe of outer medulla (*B*), and inner medulla (*C*). (*D–F*) After 30 min of dDAVP exposure, pS264 labeling increases in intensity predominantly at the apical plasma membrane, although weak basolateral plasma membrane labeling is apparent in the IMCD (*F*). (*G–L*) In comparison, total AQP2 is highly abundant in all regions before dDAVP exposure (*G–I*) but translocates to the apical membrane upon stimulation (*J–L*). (Scale bar, 10 μm.)

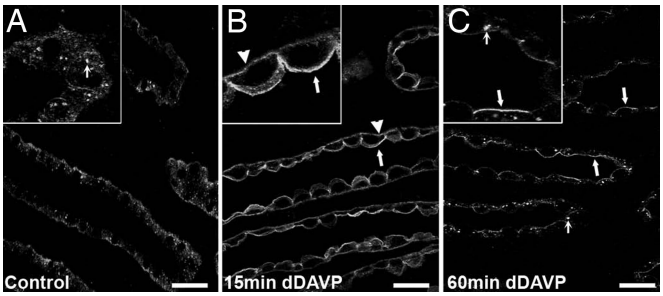

Fig. 7. Short-term vasopressin exposure results in increased pS264–AQP2 in the basolateral and apical membranes. (*A*) In control Brattleboro rats, weak intracellular labeling of pS264 is observed. In some tubules, at high magnification (*Inset*) labeling is localized to small vesicles (small arrows). (*B*) After 15 min of dDAVP treatment, pS264 labeling increases on the basolateral (arrowheads) and apical membrane (arrows); this is more apparent at high magnification (*Inset*). (*C*) After 60 min, pS264 is predominantly associated with the apical plasma membrane (arrows) and small distinct intracellular vesicles (small arrows). (Scale bars, 20 μm.)

pS264–AQP2 Is Found in Early Endosomes but Not Lysosomes After Acute AVP Treatment of Brattleboro Rats. To define the subcellular distribution of pS264–AQP2 after dDAVP treatment, double immunofluorescence labeling with anti-pS264 and known intracellular markers was performed (SI Fig. 15). At no time point examined did pS264 colocalize significantly with markers of the ER, the Golgi, or the TGN (data not shown), confirming our previous observations in Sprague–Dawley rats. Fifteen minutes after dDAVP treatment, a large increase in pS264 labeling was observed at the basolateral and apical membranes. At the apical pole of the principal cell, there was also an increased colocalization between pS264 and clathrin-coated vesicle markers (Fig. 8*B*). Sixty minutes after dDAVP treatment, the majority of pS264 labeling was associated with the apical plasma membrane, but additionally pS264 colocalized significantly with early endosome markers (Fig. 8*F*) and recycling endosome markers (data not shown). Neither at 15 nor 60 min after dDAVP treatment did we observe colocalization of pS264 with lysosomes.

Basolateral Localization of pS264–AQP2 Is Not Observed After Long-Term Increases in Circulating Vasopressin Levels. After either continuous dDAVP infusion for 5 days in Brattleboro rats or water restriction of Sprague–Dawley rats for 5 days, the majority of pS264–AQP2 labeling was observed in the apical plasma membrane throughout the CD (Fig. 9). In contrast to the acute effect of AVP, no basolateral staining and zero punctate staining of intracellular structures could be observed.

Discussion

A major physiological response of the kidney CD to AVP is to initialize the trafficking of intracellular AQP2-containing vesicles to the plasma membrane, thus increasing water permeability and urinary concentrating capacity. Although phosphorylation of AQP2 at S256 is known to play a critical role in this exocytic pathway, very little is known about the additional role of phosphorylation at S261, S264, and S269. In the current study, we used a phospho-specific antibody to examine both the acute and long-term effects of AVP on the regulation of pS264–AQP2. Our results show clearly strong increases in S264–AQP2 phosphorylation in response to AVP throughout the CD system, providing clear evidence that dynamic phosphorylation of AQP2 may play divergent roles in its subcellular distribution.

The anti-pS264 antibody used in this study successfully recognized a synthetic AQP2 peptide phosphorylated at S264 and did not cross-react with either unphosphorylated or S256-phosphorylated peptides (R.A.F., J.D.H., and M.A.K., unpublished data). Corroborating this initial characterization, preabsorption of the anti-pS264 antibody with the same synthetic pS264–AQP2 peptide completely abolished specific staining of the kidney CD. Additionally, there was a complete lack of CD labeling in AQP2 knockout mice. Taken together, these results confirm that the anti-pS264 antibody detects only pS264–AQP2.

Immunohistochemistry determined that pS264–AQP2 was present in principal cells of all CD segments from IMCD through to the cortical collecting duct, as well as cells of the CNT. In normal animals with free access to water, pS264–AQP2 distribution was consistent, with the majority of labeling being associated with the apical plasma membrane domain. An analysis of subcellular distribution demonstrated that pS264–AQP2 is not located in the ER, Golgi, or lysosomes but is associated with both the plasma membrane and endocytic retrieval compartments. The high degree of colocalization between total AQP2 and pS264–AQP2 suggests that, even under normal conditions, a large percentage of total AQP2 may be phosphorylated at this position; future studies providing a direct measurement of the percentage of total AQP2 phosphorylated at the different serine residues would be informative. In our previous study (7), the subapical punctate distribution of the pS261-AQP2 form is completely different from the distribution of the pS264–AQP2 described here, suggesting the presence of both distinct subcellular pools of AQP2 and that phosphorylation may be involved in regulating the subcellular localization of AQP2.

A major finding in the present study is the divergent regulation of pS264–AQP2 by AVP. Acute AVP exposure resulted in increased abundance of pS264–AQP2 within 30 min that remained elevated throughout the time period examined. In addition to this, we observed a time-dependent redistribution of the subcellular localization of pS264. Fifteen minutes after a single IV injection of 1 ng dDAVP, pS264–AQP2 labeling was not apparent in intracellular vesicles but was highly abundant in both the basolateral and apical membrane domains. The apparent increase in pS264–AQP2 on the basolateral membrane at the earliest time point is intriguing and could be attributable to the following: (*i*) acute trafficking of pS264–AQP2 to the basolateral membrane upon stimulation; or (*ii*) phosphorylation of a pool of AQP2 already present in the basolateral membrane. Unfortunately, our studies could not distinguish between the two possibilities. Previous studies examining the acute effect of AVP on AQP2 redistribution have not observed increased basolateral targeting of total AQP2 (8, 9). However, it is important to emphasize that in our study, the majority of basolateral pS264–AQP2 was apparent 15 min after dDAVP exposure (a much earlier time point than the previous studies) and that the antibodies used to detect total AQP2 in the previous studies are not likely to detect AQP2 phosphorylated at position 264 (J.D.H., R.A.F., and M.A.K., unpublished observations).

Sixty minutes after a single i.v. injection of dDAVP, the majority of pS264–AQP2 was associated with the apical plasma membrane and early endosomes, a small percentage was localized to recycling endosomes, and none of the pS264–AQP2 was localized to lysosomes. At this time point, decreased pS264 labeling of the basolateral membrane was observed, although the exact cause of this decrease was unknown (e.g., increased localized phosphatase activity, decreased local kinase activity, or protein degradation). Another possibility is that pS264–AQP2 is transcytosed to the apical surface from the basolateral side (10, 11). The colocalization of pS264–AQP2 with the clathrin-coated pit marker adaptin-β after 60 min suggests that a fraction of total pS264–AQP2 is present in coated pits, presumably in preparation for endocytic retrieval of AQP2 by a clathrin-mediated process (12–14). This endocytic retrieval of pS264–AQP2 was evident from its internalization into EEA1-positive early endosomes, a process that has been shown previously to occur for total AQP2 by a phosphatidylinositol 3-kinase-dependent mechanism (15). Furthermore, the appearance of pS264–AQP2 in Rab11-positive recycling vesicles suggests that

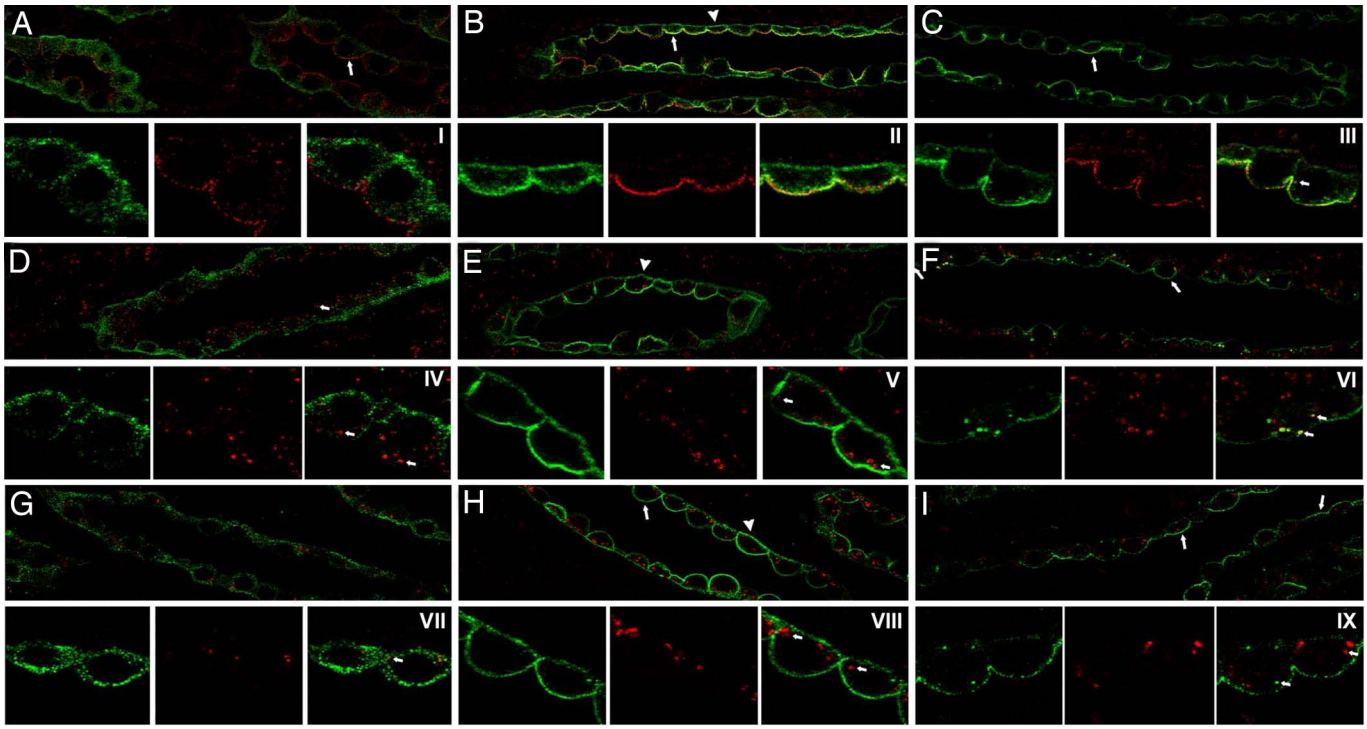

Fig. 8. Subcellular distribution of pS264–AQP2 after short-term vasopressin treatment. Brattleboro rats were treated with vehicle (15 or 60 min) or dDAVP (15 or 60 min), and double immunofluorescence labeling was performed. For all images, pS264 is depicted in green, the specific intracellular marker is depicted in red, and the overlaid images show colocalized pixels is in yellow. (*A*) Weak intracellular pS264 labeling is apparent in controls that does not colocalize with the clathrin-coated pit marker adaptin-β (arrow). (*B*) pS264 labeling increases on the basolateral (arrowheads) and apical membrane (arrows) after 15 min of dDAVP. (*C*) After 60 min, pS264 is predominantly associated with the apical plasma membrane (arrows) and small intracellular vesicles. At high magnification, this series of events is more apparent (I–III) with distinct pS264 labeling of vesicle structures at 60 min (small arrows). (*D*) pS264 labeling does not colocalize with the early endosome marker EEA1. (*E*) pS264 labeling increases on the basolateral (arrowheads) and apical membrane after 15 min of dDAVP but does not colocalize with EEA1. (*F*) After 60 min, pS264 is associated with the apical plasma membrane (arrows) and small EEA1-positive intracellular vesicles. At high magnification (IV–VI), pS264 labeling of both EEA1-positive vesicles (small arrows) and EEA1-negative vesicles is apparent after 60 min. (*G–I*) pS264 labeling does not colocalize at any time point with the lysosome marker cathepsin D. At high magnification (VII–IX), distinct pS264-positive or cathepsin D-positive vesicles are apparent (small arrows).

S264 phosphorylation may be involved in AQP2 recycling after internalization.

Although pS264–AQP2 is internalized to early endosomes, the signal for endocytosis remains unclear. It is possible that phosphorylation itself is the signal that allows AQP2 to interact with the endocytic machinery and be internalized. Indeed, it has been shown recently that pS256 is important for a direct interaction of AQP-2 with 70-kDa heat shock proteins and, ultimately, the AQP-2 shuttle (16). Moreover, recent evidence suggests that ubiquitination of the C-terminal tail of AQP2 at K270 is important for internalization (17), and it would be interesting to determine whether S264 phosphorylation can influence the level of AQP2 ubiquitination. Once ubiquitinated, AQP2 can be readily internalized, where it is transported to multivesicular bodies and targeted for proteasomal degradation. However, because pS264–AQP2 is never observed in lysosomes, it is unlikely that the proteasomal degradation pathway occurs for this phosphoform, and thus it would be interesting to examine whether pS264–AQP2 is present in urinary exosomes, an alternative pathway for excreting proteins internalized via multivesicular bodies (18).

In conclusion, this study presents, to our knowledge, the first direct evidence demonstrating AVP regulation of AQP2 phosphorylation at S264. It also shows that differentially phosphorylated forms of AQP2 can have drastically different intracellular distributions. Our findings suggest that phosphorylation of AQP2 at distinct sites may influence both AQP2 trafficking and compartmentalization; providing the clues for extensive future research into aquaporin function.

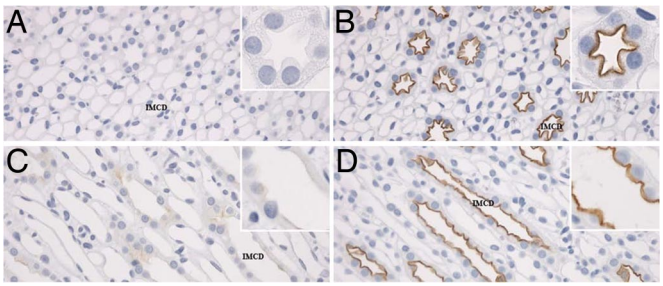

Fig. 9. Long-term increases in circulating vasopressin levels result in predominantly apical plasma membrane localization of pS264–AQP2. (*A* and *B*) Weak intracellular labeling of pS264 is evident in control Brattleboro rat kidney inner medulla (*A*) that increases in abundance at the apical plasma membrane after 5 days of continuous dDAVP infusion (*B*). (*C* and *D*) Weak intracellular pS264 labeling is apparent in the inner medulla of water-loaded Sprague–Dawley rats (*C*) that increases in abundance at the apical plasma membrane after 5 days of water restriction (*D*).

Materials and Methods

Materials. An affinity-purified rabbit polyclonal antibody (anti-pS264) was generated against a proprietary sequence from the COOH terminus of rat AQP2 that included pS264 (PhosphoSolutions). The affinity-purified antibody anti-pS256, which recognizes AQP2 phosphorylated at Ser-256, has been described previously (19). Total AQP2 antibodies were against the amino terminus (N-20, Santa Cruz Biotechnology) or the COOH terminus of rat AQP2. Initial characterization of the anti-pS264 antibody determined that the antibody was specific for the pS264–

AQP2 isoform (R.A.F., J.D.H., and M.A.K., unpublished data). The commercial antibodies used were as follows: mouse monoclonal antibodies against calbindin D-28K (Research Diagnostics); mannose-6-phosphate (AbCam); E-cadherin, PDI, early endosome associated protein (EEA1), Golgi SNARE 28 (GS28), p115, Vti1a, clathrin heavy chain, adaptin-B, adaptin-G, Rab11 (all BD Transduction Laboratories); and a goat polyclonal antibodies against cathepsin D (Research Diagnostics).

Animal Studies. The following animal protocols have been approved by the boards of the Institute of Anatomy and Institute of Clinical Medicine, University of Aarhus, according to the licenses for use of experimental animals issued by the Danish Ministry of Justice.

Protocol 1: Normal Sprague–Dawley rats, normal C57BL6J mice, and CD-specific AQP2 knockout mice. Animals were maintained on a standard rodent diet and had free access to water. CD-specific knockout mice and WT controls were originally generated by Rojek *et al.* (20). Animals were anesthetized with isoflurane and kidneys were perfusion-fixed.

Protocol 2: Short-term dDAVP infusion of Sprague–Dawley rats. Before the experiment, rats had free access to standard rat chow and water. Four rats were treated with s.c. injections of 1 ng of dDAVP (Sigma-Aldrich) in 200 μl of saline per animal, and four vehicle-injected rats served as controls. After 30 min, rats were anesthetized and kidneys were perfusion-fixed.

Protocol 3. Short-term dDAVP infusion of Brattleboro rats.

Vasopressin-deficient homozygous Brattleboro rats had free access to standard rat chow and water. Eight rats were treated with i.v. injection of 1 ng of dDAVP in 200 μl of saline per animal, and eight saline-injected rats served as controls. After 15 or 60 min, the rats (four rats for each group) were anesthetized and kidneys were perfusion-fixed. Between injection of dDAVP and fixation of the kidney, the 60-min group had free access to water but not food. The 15-min group was kept under anesthesia.

Protocol 4. Long-term dDAVP infusion of Brattleboro rats and water-loading/restriction of Sprague–Dawley rats.

Brattleboro rats had free access to standard rat chow and water and were implanted s.c. with osmotic minipumps (Altzet) delivering either 5 ng/h dDAVP or isotonic saline. After 5 days, the rats (six rats for each group) were anesthetized by halothane and kidneys were perfusion-fixed. For water-loading/restriction studies, Sprague–Dawley rats (≈200 g) were kept in metabolic cages and fed a gelled diet containing either 15 ml of water (restricted) or 45 ml of water (loaded) as described in ref. 21. After 5 days, the rats (five rats for each group) were anesthetized and kidneys were perfusion-fixed.

Immunohistochemistry and Semiquantitative Immunoblotting. For all studies, the kidneys were perfusion-fixed through the abdominal aorta and samples prepared as has been described in detail in ref. 8. For each study, a minimum of four animals were in each group to facilitate comparisons and statistical analysis where appropriate. Our immunohistochemical labeling techniques have been described in detail in ref. 8.

Colocalization Studies. For confocal laser scanning microscopy studies, the following secondary fluorescent antibodies were used at a 1:1,000 dilution: goat anti-rabbit IgG, Alexa Fluor 488; goat anti-mouse IgG, Alexa Fluor 546; goat anti-chicken IgG, Alexa Fluor 546; and donkey anti-goat IgG, Alexa Fluor 555 (Molecular Probes and Invitrogen). Laser confocal microscopy was carried out with a TCS-SP2 laser confocal microscope (Leica). To quantify the degree of colocalization, numerous high-resolution images from different experimental rat kidney sections (at least 10 images for each condition) were obtained sequentially by using a 488-nm laser line and emission between 505 and 540 nm for Alexa 488 and a 546-nm laser line and emission over 585 nm for Alexa 546/555. Background correction and quantification of colocalization was carried out by using ImageJ software.

Immunoelectron Microscopy. Lowicryl-embedded tissue blocks were prepared from perfusion-fixed kidneys, and immunogold labeling was performed as described in detail ref. 8.

ACKNOWLEDGMENTS. We thank Christian Westburg, Inger Merete Paulsen, Helle Høyer, and Zhila Nikrozi for expert technical assistance. R.A.F. is supported by a Marie Curie Intra-European Fellowship and the Danish National Research Foundation (Danmarks Grundforskningsfond). The Water and Salt Research Center at the University of Aarhus is established and supported by the Danish National Research Foundation (Danmarks Grundforskningsfond). Further support for this study was provided by The Nordic Centre of Excellence (NCoE) Program in Molecular Medicine and by a European Union Marie Curie Training Network Program. M.A.K. received funding from the Intramural Budget of the National Heart, Lung, and Blood Institute (National Institutes of Health Grant Z01-HL001285).

1. Nielsen S, *et al.* (2002) Aquaporins in the kidney: from molecules to medicine. *Physiol Rev* 82:205–244.
2. Fushimi K, Sasaki S, Marumo F (1997) Phosphorylation of serine 256 is required for cAMP-dependent regulatory exocytosis of the aquaporin-2 water channel. *J Biol Chem* 272:14800–14804.
3. Katsura T, Gustafson CE, Ausiello DA, Brown D (1997) Protein kinase A phosphorylation is involved in regulated exocytosis of aquaporin-2 in transfected LLC-PK1 cells. *Am J Physiol* 272:F817–F822.
4. Kamsteeg EJ, Heijnen I, van Os CH, Deen PM (2000) The subcellular localization of an aquaporin-2 tetramer depends on the stoichiometry of phosphorylated and nonphosphorylated monomers. *J Cell Biol* 151:919–930.
5. McDill BW, *et al.* (2006) Congenital progressive hydronephrosis (cph) is caused by an S256L mutation in aquaporin-2 that affects its phosphorylation and apical membrane accumulation. *Proc Natl Acad Sci* USA 103:6952–6957.
6. Hoffert JD, *et al.* (2006) Quantitative phosphoproteomics of vasopressin-sensitive renal cells: regulation of aquaporin-2 phosphorylation at two sites. *Proc Natl Acad Sci USA* 103:7159–7164.
7. Hoffert JD, *et al.* (2007) Dynamics of aquaporin-2 serine-261 phosphorylation in response to short-term vasopressin treatment in collecting duct. *Am J Physiol Renal Physiol* 292:F691–F700.
8. Christensen BM, Wang W, Frokiaer J, Nielsen S (2003) Axial heterogeneity in basolateral AQP2 localization in rat kidney: Effect of vasopressin. *Am J Physiol Renal Physiol* 284:F701–F717.
9. Jeon US, *et al.* (2003) Oxytocin induces apical and basolateral redistribution of aquaporin-2 in rat kidney. *Nephron Exp Nephrol* 93:e36–e45.
10. Rodriguez-Boulan E, Kreitzer G, Musch A (2005) Organization of vesicular trafficking in epithelia. *Nat Rev Mol Cell Biol* 6:233–247.
11. Breuza L, Monlauzeur L, Arsanto JP, Le Bivic A (1999) Identification of signals and mechanisms of sorting of plasma membrane proteins in intestinal epithelial cells. *J Soc Biol* 193:131–134.
12. Lu H, *et al.* (2004) Inhibition of endocytosis causes phosphorylation (S256)-independent plasma membrane accumulation of AQP2. *Am J Physiol Renal Physiol* 286:F233–F243.
13. Bouley R, *et al.* (2006) Aquaporin 2 (AQP2) and vasopressin type 2 receptor (V2R) endocytosis in kidney epithelial cells: AQP2 is located in ''endocytosis-resistant'' membrane domains after vasopressin treatment. *Biol Cell* 98:215–232.
14. Russo LM, McKee M, Brown D (2006) Methyl-beta-cyclodextrin induces vasopressin-independent apical accumulation of aquaporin-2 in the isolated, perfused rat kidney. *Am J Physiol Renal Physiol* 291:F246–F253.
15. Tajika Y, *et al.* (2004) Aquaporin-2 is retrieved to the apical storage compartment via early endosomes and phosphatidylinositol 3-kinase-dependent pathway. *Endocrinology* 145:4375–4383.
16. Lu HA, *et al.* (2007) Heat shock protein 70 interacts with aquaporin-2 (AQP2) and regulates its trafficking. *J Biol Chem* 282:28721–28732.
17. Kamsteeg EJ, *et al.* (2006) Short-chain ubiquitination mediates the regulated endocytosis of the aquaporin-2 water channel. *Proc Natl Acad Sci USA* 103:18344–18349.
18. Pisitkun T, Shen RF, Knepper MA (2004) Identification and proteomic profiling of exosomes in human urine. *Proc Natl Acad Sci USA* 101:13368–13373.
19. Nishimoto G, *et al.* (1999) Arginine vasopressin stimulates phosphorylation of aquaporin-2 in rat renal tissue. *Am J Physiol* 276:F254–F259.
20. Rojek A, *et al.* (2006) Severe urinary concentrating defect in renal collecting duct-selective AQP2 conditional-knockout mice. *Proc Natl Acad Sci USA* 103:6037–6042.
21. Kim GH, *et al.* (1999) Vasopressin increases Na-K-2Cl cotransporter expression in thick ascending limb of Henle's loop. *Am J Physiol* 276:F96–F103.